

See discussions, stats, and author profiles for this publication at: <https://www.researchgate.net/publication/261189182>

In situ synthesis of Nanocomposite Membranes: Comprehensive Improvement Strategy for Direct Methanol Fuel Cells

ARTICLE in CHEMSUSCHEM · MARCH 2014

Impact Factor: 7.66 · DOI: 10.1002/cssc.201301060 · Source: PubMed

CITATIONS

11

READS

34

6 AUTHORS, INCLUDING:



Siyuan Rao

Beihang University(BUAA)

7 PUBLICATIONS 24 CITATIONS

[SEE PROFILE](#)



Shanfu Lu

Beihang University(BUAA)

57 PUBLICATIONS 1,342 CITATIONS

[SEE PROFILE](#)



Yan Xiang

Independent Researcher

74 PUBLICATIONS 646 CITATIONS

[SEE PROFILE](#)

DOI: 10.1002/cssc.201301060

In situ synthesis of Nanocomposite Membranes: Comprehensive Improvement Strategy for Direct Methanol Fuel Cells

Siyuan Rao,^[a] Ruijie Xiu,^[a] Jiangju Si,^[a] Shanfu Lu,^{*[a, b]} Meng Yang,^[a] and Yan Xiang^{*[a, b]}

In situ synthesis is a powerful approach to control nanoparticle formation and consequently confers extraordinary properties upon composite membranes relative to conventional doping methods. Herein, uniform nanoparticles of cesium hydrogen salts of phosphotungstic acid (CsPW) are controllably synthesized in situ in Nafion to form CsPW–Nafion nanocomposite

membranes with both improved proton conductivity and methanol-crossover suppression. A 101.3% increase of maximum power density has been achieved relative to pristine Nafion in a direct methanol fuel cell (DMFC), indicating a potential pathway for large-scale fabrication of DMFC alternative membranes.

Introduction

Natural materials and systems establish their fundamental units on a nanoscale level. Manipulation of materials at this level may tailor their basic properties and expand the performance of existing materials.^[1] Therefore, nanoscale materials may exhibit new or significantly improved physical and chemical properties relative to bulk or macroscale materials owing to the benefits of diminishing size.^[2] For instance, composite membranes with uniformly distributed nanoparticles show important transformations or improvement in properties, whereas the surrounding polymer chains serve as stabilizing agents and dispersants.^[3]

Methanol permeability is a common issue for direct methanol fuel cells (DMFCs) that not only results in fuel wastage, but also impairs fuel-cell performance.^[4] Introducing nanoparticles into Nafion polymers may be an effective tool to suppress methanol crossover, but is often accompanied by the loss of proton conductivity because protons and methanol are transported through the same pathway in Nafion.^[4a, 5] As an inorganic proton conductor, phosphotungstic acid ($H_3PW_{12}O_{40}$, HPW) is intensively applied to improve proton conductivity; nevertheless, a solution for fuel crossover has not yet been

found.^[5b, 6] In addition, additives fabricated by conventional methods always generate relatively large particle sizes, which could cause heterogeneity in the final preparation of composite membranes. Such heterogeneities may lead to decline in both proton conductivity and mechanical properties and consequently deterioration of fuel-cell performance.^[7] Thus, the goal of an ideal DMFC membrane with improved proton conductivity and suppressed methanol crossover still remains challenging.

In situ synthesis is a powerful approach to control nanoparticle formation and consequently achieve controllable size, compatible blends, and uniform dispersion relative to conventional doping methods.^[8] In this regard, synthesizing proton-conductive nanoparticles within a Nafion polymer matrix by an in situ approach could provide adaptive methanol barriers in diffusion channels as well as maintain sufficient proton conductivity.

Herein, nanoparticles of cesium hydrogen salts of phosphotungstic acid (CsPW) are synthesized in situ in Nafion to develop CsPW–Nafion nanocomposite membranes. With the benefit of stable nanoparticle size and uniform dispersion throughout the membrane, CsPW–Nafion nanocomposite membranes present desirable methanol-crossover suppression with improved proton conductivity. A 101.3% increase of maximum power density relative to pristine Nafion demonstrates its feasibility on potential applications in DMFCs.

Results and Discussion

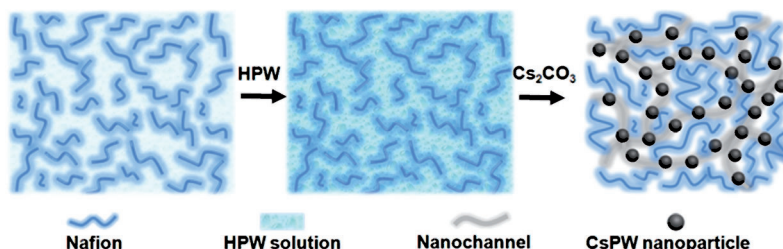
As one of the most powerful approaches to control nanoparticle formation and promote high dispersion,^[6b, 8a, 9] the in situ technique was applied to synthesize CsPW nanoparticles within a Nafion polymer matrix (Scheme 1). CsPW nanoparticles are formed through chemical reactions among Nafion polymer chains, which serve as nanoreactors for particle formation (see the Supporting Information, Figures S1 and S2).^[10] Nafion polymer chains play important roles in inhibiting the

[a] Dr. S. Rao,⁺ Dr. R. Xiu,⁺ Dr. J. Si, Prof. S. Lu, Dr. M. Yang, Prof. Y. Xiang
Beijing Key Laboratory of Bio-Inspired Energy Materials and Devices
School of Chemistry and Environment
Beihang University
100191, Beijing (PR China)
E-mail: xiangy@buaa.edu.cn
lusf@buaa.edu.cn

[b] Prof. S. Lu, Prof. Y. Xiang
Key Laboratory of Bio-Inspired Smart Interfacial Science and Technology of
Ministry of Education
School of Chemistry and Environment
Beihang University
100191, Beijing (PR China)

[+] These authors contributed equally to this work.

 Supporting Information for this article is available on the WWW under
<http://dx.doi.org/10.1002/cssc.201301060>.



Scheme 1. In situ synthesis of CsPW–Nafion nanocomposite membranes. HPW was sufficiently mixed with Nafion in solution prior to synthesis. After addition of Cs_2CO_3 , CsPW nanoparticles were formed within the Nafion chains, which serve as nanoreactors. The surrounding polymer plays an important role in controlling particle size and dispersion.

growth of large CsPW particles and promoting high dispersion. The distribution and size of CsPW particles in the nanocomposite membrane were examined by TEM analysis, high-resolution transmission electron microscopy (HRTEM), and energy-dispersive X-ray (EDX) spectroscopy. Nanoscale CsPW particles are well dispersed and have homogeneous sizes: (2.87 ± 0.48) nm for 1% CsPW, (3.46 ± 0.04) nm for 5% CsPW, and (4.08 ± 0.05) nm for 10% CsPW (Figure 1). By contrast, CsPW particles synthesized ex situ in aqueous solutions without Nafion have microscale diameters (see the Supporting Information, Figure S3). These results could be explained by the function of the polymer surroundings during particle synthesis. On the one hand, chemical reactions for CsPW-particle synthesis take place among polymer chains, which would limit particle aggregation and thus yield uniform and well-dispersed nanoparticles.^[11] On the other hand, the polymer chains could also restrict the movement of formed nanoparticles and improve their stability.^[11,12] TEM and EDX analyses indicate that CsPW nanoparticles are homogeneously distributed (see the Supporting Information, Figure S4). The average diameters of the particles are in the nanometer range and slightly increase with increasing CsPW content. Under relatively high Nafion concentrations, nanoparticles are expected to have smaller sizes, which could be attributed to the large number of polymer chains avail-

able for improving particle stabilization and monodispersity.^[13] Considering that the reported water nanochannels in Nafion are <5 nm in size,^[14] the CsPW nanoparticles would be adapted to the dimensions of nanochannels to provide fundamental tailoring ability for proton transport and methanol-crossover nanoscope structures.

Because of the small size of particles distributed homogeneously, CsPW–Nafion nanocomposite membranes have a transparent appearance (Figure 2a). SEM and EDX images illustrate that the CsPW–Nafion membranes have a smooth surface and homogeneous CsPW distribution (Figure 2b and c). Unlike

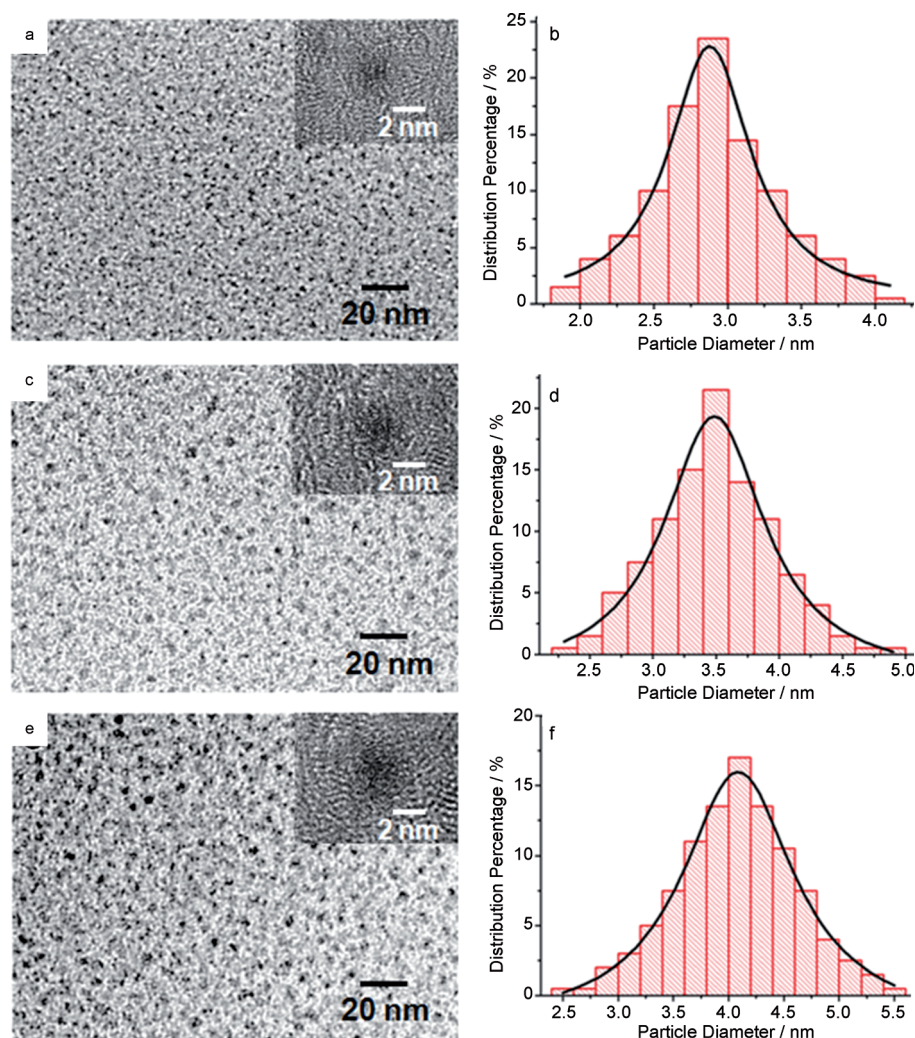


Figure 1. TEM and HRTEM analyses of CsPW–Nafion nanocomposite membranes. The distribution and size of CsPW particles in a,b) 1; c,d) 5; and e,f) 10 wt % CsPW–Nafion membranes. Inset: HRTEM profiles of synthetic nanoparticles. Nanoscale CsPW particles with uniform sizes are homogeneously distributed in Nafion. The diameter of CsPW particles is (2.87 ± 0.48) nm in the 1 wt % CsPW–Nafion membrane, (3.46 ± 0.04) nm in the 5 wt % CsPW–Nafion membrane, and (4.08 ± 0.05) nm in the 10 wt % CsPW–Nafion membrane. About 200 sample particles were counted.

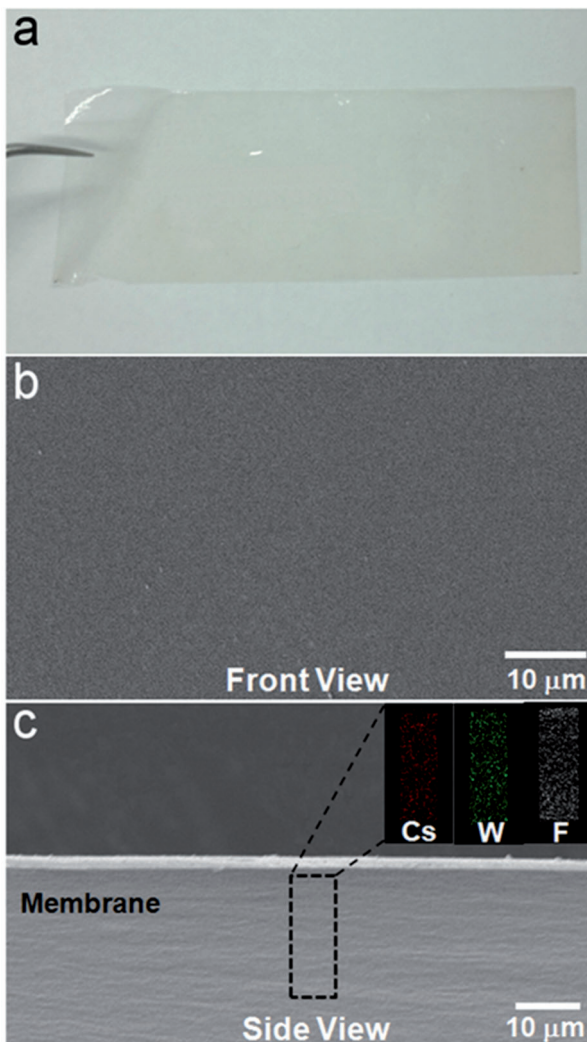


Figure 2. Morphology of CsPW–Nafion membranes: a) transparent CsPW–Nafion membrane; b) SEM and c) EDX images of the front and side views of a CsPW–Nafion membrane, which show the smooth surface and homogeneous cross-section morphology. EDX mapping of Cs, W, and F is shown in insets in (c).

ex situ synthesis, which causes phase splitting and property isotropy in the composite membrane (see the Supporting Information, Figure S5), in situ synthesis allows the controllable formation of nanoparticles and uniform dispersion within the composite membrane. XRD measurements of composite membranes indicate low crystallization of CsPW and its good distribution in the membrane (see the Supporting Information, Figure S6). FTIR measurements show that the CsPW–Nafion nanocomposite membranes possess well-preserved HPW structures (see the Supporting Information, Figure S7). Thermogravimetric (TG) and tensile strength analyses demonstrate that CsPW–Nafion membranes have sufficient thermal stability (see the Supporting Information, Figure S8) and good mechanical properties (see the Supporting Information, Table S1). Interface combination and water management are important to fuel-cell performance; thus, the surface properties of the membranes were investigated by atomic force microscopy (AFM) and

water contact angle examination. Solutions of CsPW–Nafion membranes were cast on mica and then examined by AFM analysis. Figure 3a–d shows typical images obtained from the cast films of recast Nafion (Re-Nafion) and CsPW–Nafion nanocomposite membranes. The roughness of each nanocomposite membrane has a linear relationship with CsPW content (Figure 3e). CsPW–Nafion membranes also exhibit increasing water contact angles in proportion to CsPW content, which indicates a gradual increase in hydrophobicity (Figure 3f). These results could be ascribed to enhancements in the surface roughness of the membranes,^[15] which results from the growing size of CsPW nanoparticles.

Additionally, proton conductivity and methanol permeability could be regulated by CsPW–nanoparticle content (Figure 4). The proton conductivity of Re-Nafion and CsPW–Nafion membranes was measured at room temperature using the four-point probe technique. An ascending tendency with increasing CsPW content was observed (Figure 4a). The proton conductivity of the Re-Nafion membrane was $3.95 \times 10^{-2} \text{ mS cm}^{-1}$. By comparison, CsPW–Nafion nanocomposite membranes exhibit superior conductivities of $4.90 \times 10^{-2} \text{ mS cm}^{-1}$ for the 1 wt% CsPW–Nafion membrane, $5.02 \times 10^{-2} \text{ mS cm}^{-1}$ for the 5 wt% CsPW–Nafion membrane, and $7.25 \times 10^{-2} \text{ mS cm}^{-1}$ for the 10 wt% CsPW–Nafion membrane. Protons diffuse through Nafion nanochannels freely, which results in a high conductivity. Generally, water in hydrophilic domains and interactions between cations and sulfonic acid groups would affect the proton conductivity of composite membranes.^[7] In Nafion composite membranes doped with other nanoparticles,^[16] such as SiO₂ and ZrO₂, water uptake is mostly considered to enhance proton conductivity especially at higher temperatures. In fact, the insulating particles themselves act as proton barriers leading to a decrease in proton conductivity. Upon introduction of the water-holding Keggin structure of CsPW with outstanding proton conductivity,^[17] more water could be retained inside the channels and proton mobility in the membrane would be enhanced (Figure 4c). Nanoscale CsPW particles with large surface areas and pore volumes could provide additional functional sites for proton conduction.^[18] By contrast, large particles synthesized by the ex situ approach have detrimental effects on proton conductivity (see the Supporting Information, Table S2) because of the deterioration of inherent Nafion proton-transport nanochannels.

CsPW nanoparticles synthesized in situ can achieve effective reduction of methanol crossover in composite membranes. The methanol permeability of the membranes was evaluated through methanol diffusion coefficient measurements. The results in Figure 4b show the appreciable improvement of methanol-crossover suppression of CsPW–Nafion membranes relative to the Re-Nafion membrane. The Re-Nafion membrane presents a diffusion coefficient ($6.64 \times 10^{-7} \text{ cm}^2 \text{s}^{-1}$) that is much higher than that of all of the other CsPW–Nafion membranes. Methanol-permeability measurements were conducted in a homemade cell with an initial 2 M methanol solution. Diffusion coefficients further decrease with increasing CsPW content ($4.32 \times 10^{-7} \text{ cm}^2 \text{s}^{-1}$ for the 1 wt% CsPW–Nafion membrane, $1.54 \times 10^{-7} \text{ cm}^2 \text{s}^{-1}$ for the 5 wt% CsPW–Nafion mem-

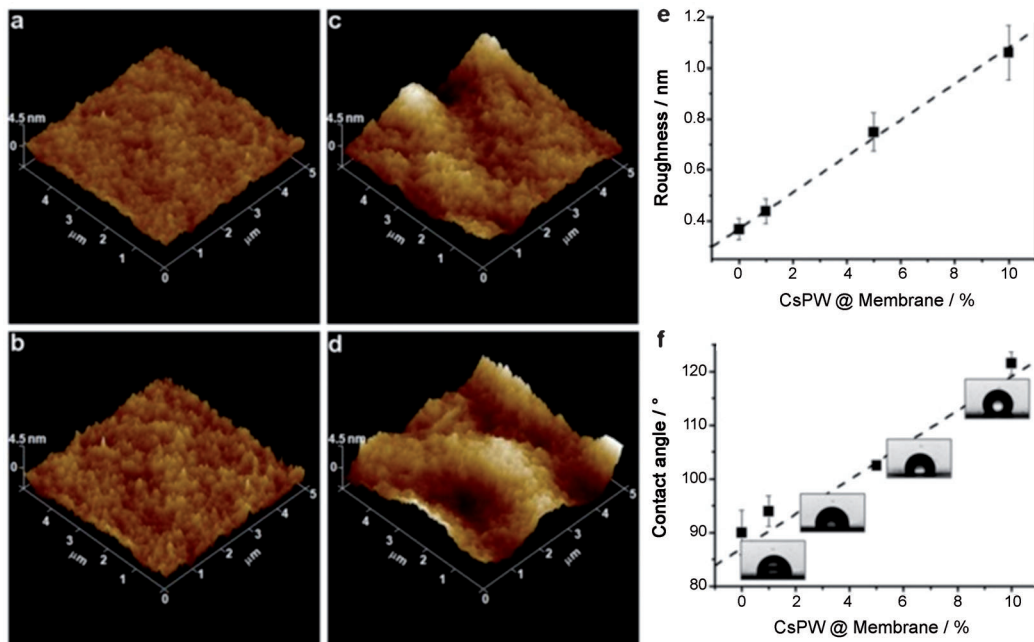


Figure 3. Surface roughness and wettability of Re-Nafion and CsPW–Nafion membranes. a–d) AFM images of Re-Nafion and CsPW–Nafion membranes; e) surface roughness of each membrane shows a linear relationship with CsPW content; f) water contact angles on membrane surfaces increase in proportion to CsPW content, which indicates enhanced hydrophobicity.

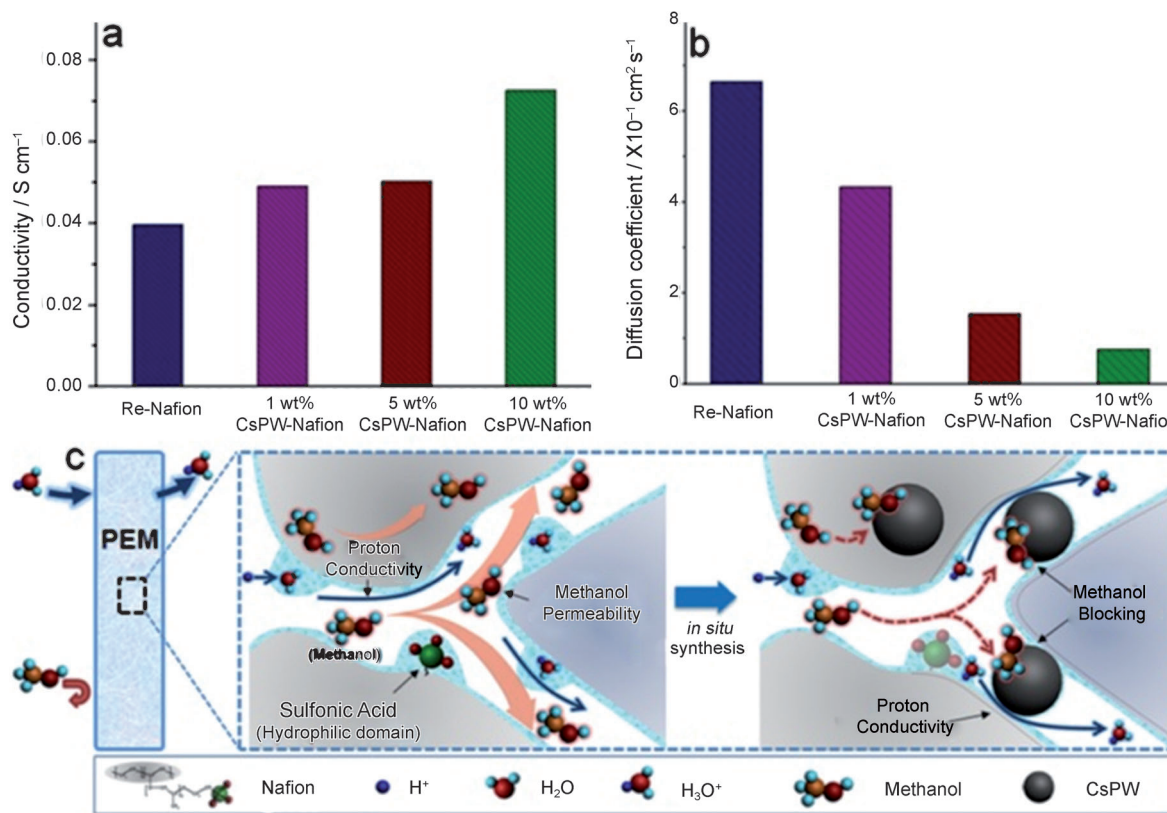


Figure 4. Proton conductivity and methanol permeability of Re-Nafion and CsPW–Nafion membranes and their proposed mechanisms. a) Proton conductivity of the CsPW–Nafion membrane synthesized *in situ* increases with increasing CsPW content, which indicates the favorable effects of *in situ* synthesis; b) methanol diffusion coefficient decreases dramatically with increasing CsPW content, which suggests effective methanol-crossover suppression. The initial methanol concentration is 2 mol L⁻¹; c) mechanisms of proton transport and methanol-crossover suppression in the CsPW–Nafion film synthesized *in situ*.

brane, and $7.53 \times 10^{-8} \text{ cm}^2 \text{s}^{-1}$ for the 10 wt% CsPW–Nafion membrane), which reveals enhanced methanol-crossover suppression effects. The limiting methanol-permeation current density, which may be obtained from the oxidation reaction in the working electrode by electrochemical measurements, displays similar tendencies (see the Supporting Information, Figure S9) and further demonstrates significant improvement in methanol blocking by CsPW–nanoparticle addition. Methanol molecules migrate from the anode to the cathode through Nafion nanochannels, causing methanol permeation. During *in situ* synthesis, nm-scale CsPW nanoparticles are formed in a controllable manner and are homogeneously distributed through the Nafion polymer. By this synthesis approach, particle dimensions would be adapted to the methanol-diffusion nanochannels, and the CsPW nanoparticles could serve as good methanol barriers (Figure 4c). Conventional CsPW particles synthesized *ex situ* have large sizes and cause severe aggregation in the final composite membrane, which damages the intrinsic Nafion nanochannel structures. Such damage is detrimental to methanol blocking (see the Supporting Information, Table S2). In addition, the extraordinary architecture of heteropolyacids and enhanced interactions between HPW anions and sulfonic acid groups could also promote the absorption of methanol molecules and reductions in channel size, thereby providing support for methanol blocking.^[19]

The comprehensive performance of CsPW–Nafion nanocomposite membranes synthesized *in situ* and applied in DMFCs was evaluated by single-cell tests. As shown in Figure 5a, 1, 5, and 10 wt% CsPW–Nafion membranes exhibit increases of 30.1%, 101.6%, and 80.8% in maximum power density, respectively, relative to the Re-Nafion membrane. This significant increase in fuel-cell-output performance is mainly attributed to the effective suppression of methanol crossover and appreciable improvement in proton conductivity by the membranes synthesized *in situ*. The fuel cell with the 5 wt% CsPW–Nafion membrane shows optimum performance with a maximum power density of 30.6 mW cm^{-2} . Although the 10 wt% CsPW–Nafion membrane demonstrates advantages in proton conductivity and methanol blocking, the drop in its cell performance relative to the 5 wt% membrane is likely due to the comprehensive effect of the interface properties of the membrane electrode assembly (MEA) as well as the deterioration of the membrane mechanical behavior.^[7] Large amounts of inorganic additives and increasing particle sizes could cause the decrease of membrane mechanical properties (see the Supporting Information, Table S1) and a rougher surface (Figure 3), which is harmful to the integration of catalysts in the electrodes and water management. During long-term cycling tests, the composite membranes exhibit a highly stable conductivity (Figure 5b). Overall, benefiting from the multiple advantages of CsPW particles synthesized *in situ*, the nanocomposite membranes show significant improvement in cell performance.

Conclusions

Through *in situ* synthesis, CsPW–Nafion nanocomposite membranes are successfully fabricated and applied in DMFCs. Bene-

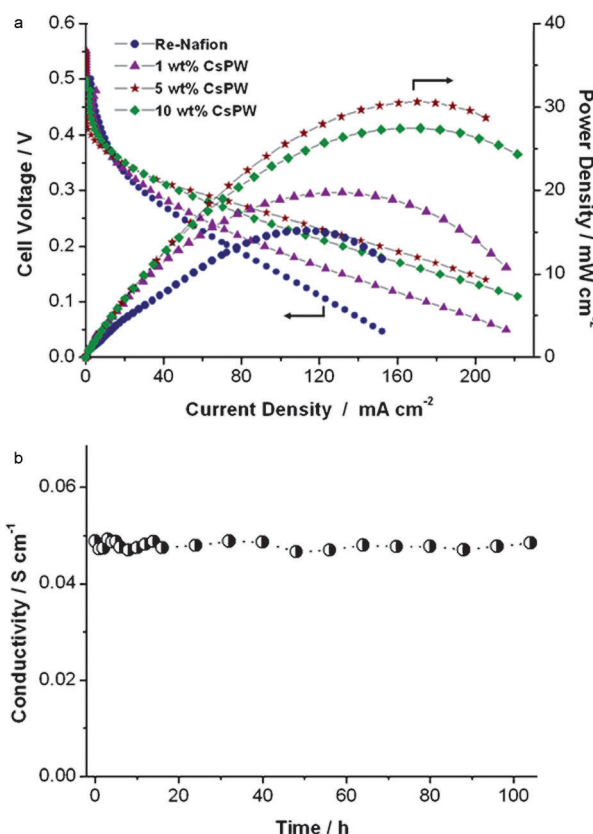


Figure 5. DMFC single-cell performance and membrane conductivity stability tests: (a) single-cell test of Re-Nafion and CsPW–Nafion DMFCs conducted at 25°C with 2 mol L^{-1} methanol at the anode and 100 sccm O_2 at the cathode. CsPW–Nafion DMFCs have improved power density relative to the Re-Nafion DMFC; b) membrane-conductivity stability is evaluated by the four-point probe technique for 104 h with the 5 wt% CsPW–Nafion membrane. There is no clear loss in conductivity, which indicates the good stability of the membrane.

fiting from the uniformity and homogeneous distribution of CsPW nanoparticles, nanocomposite membranes exhibit significant methanol-crossover suppression and maintain substantial proton conductivity. A maximum power density improvement of 101.6% is achieved in cell-performance tests. These findings indicate a simplified and optimized pathway for fabrication of DMFC alternative membranes potentially on an industrial scale.

Experimental Section

Materials

Nafion solution (5 wt%) was supplied by DuPont. Cesium carbonate and phosphotungstic acid hydrate ($\text{H}_3\text{PW}_{12}\text{O}_{40} \cdot n\text{H}_2\text{O}$) were purchased from Sigma-Aldrich. Methanol was obtained from Fluka. All reagents used herein were of analytical grade and did not require further purification. All aqueous solutions were prepared using ultrapure water (Millipore, $18.2 \text{ M}\Omega \text{ cm}$ at 25°C).

Preparation of CsPW–Nafion nanocomposite membranes

$\text{Cs}_{2.5}\text{H}_{0.5}\text{PW}_{12}\text{O}_{40}/\text{Nafion}$ (CsPW–Nafion) nanocomposite membranes were prepared at three CsPW contents (1, 5, and 10 wt%) by

in situ synthesis and recasting. According to the CsPW synthesis reaction,^[10,20] CsPW nanoparticles were in situ synthesized by adding Cs₂CO₃ (0.05 mol L⁻¹) dropwise into a mixture of HPW (0.1 mol L⁻¹) and Nafion (5 wt %) with corresponding molar ratio of reactants (*n*(Cs₂CO₃):*n*(HPW) = 5:4). Ultrasonic vibration was applied to avoid particle aggregation. After casting onto clean glass dishes, the membranes were evaporated at 60, 80, 100, and 120 °C for 8 h before finally cooling to room temperature. Dried membranes with an average thickness of 50 µm were peeled off from the glass. A Re-Nafion membrane was prepared using the same procedures.

Characterization

CsPW nanoparticles synthesized in situ in Nafion were examined by TEM analysis (Philips, TECNAI-20). The surface morphology of CsPW–Nafion membranes was examined using an environmental scanning electron microscope (ESEM, FEI QUANTA 250) at an acceleration voltage of 3 kV and a reduced pressure of 70 Pa. All samples were precoated with a gold layer by sputtering before observation to avoid charging under the electron beam. AFM analyses were conducted using a Dimension Icon instrument (Bruker, USA) and water contact angles were measured on the surface of CsPW–Nafion membranes using an OCA20 (DataPhysics, Germany) contact-angle-measuring instrument. At least five points on a single surface were recorded to obtain a mean value. FTIR spectra were recorded on a NICOLET 750 spectrophotometer in the range of 2000–650 cm⁻¹ at a resolution of 2 cm⁻¹ in absorbance mode. The thermal stability of all samples was assessed by TG and derivative TG analyses (DTG) using a Netzsch Sta 409 C/CD instrument (German). Samples weighing between 5 and 10 mg were heated from 25 to 600 °C at a rate of 10 °C min⁻¹, while the apparatus was continually flushed with a nitrogen flow of 30 mL min⁻¹.

Proton conductivity

The proton conductivity of CsPW–Nafion membranes was measured by the four-point probe technique. The impedance of the samples was determined using a potentiostat/galvanostat/frequency-response analyzer (PARSTAT 2273) at room temperature and frequencies ranging from 100 kHz to 1 Hz with an amplitude voltage of 10 mV. The proton conductivity (σ) of the membranes was calculated according to Equation (1):

$$\sigma = \frac{L}{RS} \quad (1)$$

where L , R , and S are the membrane thickness (cm), measured resistance (Ω), and membrane surface area (cm²) of the samples, respectively.

Methanol permeability

The methanol permeability of CsPW–Nafion membranes was measured in a homemade cell. The cell was separated into two compartments by the membrane. The initial concentration of methanol in one of the compartments was 2 mol L⁻¹, and the other compartment contained ultrapure water. The solution in each cell compartment was stirred continuously during permeability measurement. The increase in methanol concentration over time was detected using an Agilent GC 6890N gas chromatograph equipped with an HP-PLOT/U column.

Single-cell tests

To evaluate the performance of the DMFCs, a MEA was constructed by sandwiching individual CsPW membranes between a Pt–Ru black (E-TEK) anode and a Pt black (E-TEK) cathode. The loading amounts of Pt in the catalyst layers impregnated with a Nafion solution (5%) were 4.0 and 1.0 mg cm⁻² in the anode and cathode layers, respectively. The MEA was hot-pressed at 135 °C and 4 MPa for 90 s. Prior to each test, the cell was fed by a methanol solution (2 mol L⁻¹) for 24 h at 80 °C. The cathode was dried in a N₂ atmosphere at a flow rate of 200 sccm after cooling to room temperature. The single-cell performance was measured at room temperature (25 °C) with a methanol solution (2 mol L⁻¹) at the anode and 100 sccm O₂ at the cathode.

Acknowledgements

This work was financially supported by grants from the National Natural Science Foundation of China (No. 21003007, U1137602, 21073010, 51108014), National High Technology Research and Development Program of China (863 program, 2013AA031902), the National Research Fund for Fundamental Key Projects (973 Program) (No. 2011CB935700), National Science Foundation of Beijing (No. 2132051), Program for New Century Excellent Talents in University (NCET-10-0038) and the Fundamental Research Funds for the Central Universities (YWF-13-T-RSC-030). We thank Dr. J. Zhang (Curtin University) for beneficial discussions.

Keywords: electrochemistry • fuel cells • membranes • nanoparticles • polymers

- [1] A. C. Balazs, T. Emrick, T. P. Russell, *Science* **2006**, *314*, 1107–1110.
- [2] a) Y. Zhao, K. Thorkelsson, A. J. Mastrianni, T. Schilling, J. M. Luther, B. J. Rancatore, K. Matsunaga, H. Jinnai, Y. Wu, D. Poulsen, *Nat. Mater.* **2009**, *8*, 979–985; b) A. J. Crosby, J. Y. Lee, *Polym. Rev.* **2007**, *47*, 217–229; c) D. S. Su, R. Schlögl, *ChemSusChem* **2010**, *3*, 136–168; d) M. Dou, M. Hou, H. Zhang, G. Li, W. Lu, Z. Wei, Z. Shao, B. Yi, *ChemSusChem* **2012**, *5*, 945–951; e) C.-H. Cui, H.-H. Li, S.-H. Yu, *Chem. Sci.* **2011**, *2*, 1611–1614; f) Z. M. Cui, S. P. Jiang, C. M. Li, *Chem. Commun.* **2011**, *47*, 8418–8420; g) M.-R. Gao, Y.-F. Xu, J. Jiang, S.-H. Yu, *Chem. Soc. Rev.* **2013**, *42*, 2986–3017; h) M.-R. Gao, Q. Gao, J. Jiang, C.-H. Cui, W.-T. Yao, S.-H. Yu, *Angew. Chem.* **2011**, *123*, 5007–5010; *Angew. Chem. Int. Ed.* **2011**, *50*, 4905–4908.
- [3] a) H. Oh, P. F. Green, *Nat. Mater.* **2009**, *8*, 139–143; b) G. Schmidt, M. M. Malwitz, *Curr. Opin. Colloid Interface Sci.* **2003**, *8*, 103–108; c) M. A. López-Quijada, *Curr. Opin. Colloid Interface Sci.* **2003**, *8*, 137–144; d) J. Li, H. Tang, L. Chen, R. Chen, M. Pan, *Chem. Commun.* **2013**, *49*, 6537–6539; e) J. Lu, H. Tang, S. Lu, H. Wu, S. P. Jiang, *J. Mater. Chem.* **2011**, *21*, 6668–6676.
- [4] a) Y. Xiang, S. Lu, *Chem. Soc. Rev.* **2012**, *41*, 7291–7321; b) B. Gurau, E. S. Smotkin, *J. Power Sources* **2002**, *112*, 339–352.
- [5] a) J. Zhang, F. Lan, D. Liang, Y. Xiao, S. Lu, Y. Xiang, *J. Membr. Sci.* **2011**, *382*, 350–354; b) M. Yang, S. Lu, J. Lu, Y. Xiang, *Chem. Commun.* **2010**, *46*, 1434–1436.
- [6] a) S. Lu, D. Wang, S. P. Jiang, Y. Xiang, J. Lu, J. Zeng, *Adv. Mater.* **2010**, *22*, 971–976; b) Z. Chen, B. Holmberg, W. Li, X. Wang, W. Deng, R. Munoz, Y. Yan, *Chem. Mater.* **2006**, *18*, 5669–5675; c) H. Tang, C. Liang, J. Li, H. Zhang, H. Zhang, M. Pan, *J. Mater. Chem. A* **2013**, *2*, 753–760.
- [7] N. W. Deluca, Y. A. Elabd, *J. Polym. Sci. Part B* **2006**, *44*, 2201–2225.
- [8] a) H. Zhang, P. K. Shen, *Chem. Rev.* **2012**, *112*, 2780–2832; b) H. Tang, Z. Wan, M. Pan, S. P. Jiang, *Electrochim. Commun.* **2007**, *9*, 2003–2008; c) M.-R. Gao, S. Liu, J. Jiang, C.-H. Cui, W.-T. Yao, S.-H. Yu, *J. Mater. Chem.* **2010**, *20*, 9355–9361.
- [9] J. J. Vilatela, D. Eder, *ChemSusChem* **2012**, *5*, 456–478.

- [10] T. Okuhara, M. Yamashita, K. Na, M. Misono, *Chem. Lett.* **1994**, 1451–1454.
- [11] L. Shang, Y. Wang, L. Huang, S. Dong, *Langmuir* **2007**, *23*, 7738–7744.
- [12] C.-W. Chen, T. Takezako, K. Yamamoto, T. Serizawa, M. Akashi, *Colloids Surf. A* **2000**, *169*, 107–116.
- [13] a) Z. Cui, W. Xing, C. Liu, J. Liao, H. Zhang, *J. Power Sources* **2009**, *188*, 24–29; b) S. Si, A. Kotal, T. K. Mandal, S. Giri, H. Nakamura, T. Kohara, *Chem. Mater.* **2004**, *16*, 3489–3496.
- [14] K. Schmidt-Rohr, Q. Chen, *Nat. Mater.* **2008**, *7*, 75–83.
- [15] F. Xia, L. Jiang, *Adv. Mater.* **2008**, *20*, 2842–2858.
- [16] a) C. C. Ke, X. J. Li, S. G. Qu, Z. G. Shao, B. L. Yi, *Polym. Adv. Technol.* **2012**, *23*, 92–98; b) N. H. Jalani, K. Dunn, R. Datta, *Electrochim. Acta* **2005**, *51*, 553–560.
- [17] a) P. Chen, C. Chiu, C. Hong, *J. Electrochem. Soc.* **2008**, *155*, B1255; b) C. E. Tsai, B. J. Hwang, *Fuel Cells* **2007**, *7*, 408–416.
- [18] S. Oh, T. Yoshida, G. Kawamura, H. Muto, M. Sakai, A. Matsuda, *J. Power Sources* **2010**, *195*, 5822–5828.
- [19] a) M. Helen, B. Viswanathan, S. S. Murthy, *J. Appl. Polym. Sci.* **2010**, *116*, 3437–3447; b) A. Ismail, N. Othman, A. Mustafa, *J. Membr. Sci.* **2009**, *329*, 18–29.
- [20] K. Na, T. Izaki, T. Okuhara, M. Misono, *J. Mol. Catal. A* **1997**, *115*, 449–455.

Received: October 6, 2013

Revised: November 11, 2013

Published online on February 13, 2014